

AUTOMATIC HEIGHT EXTRACTION FROM ERS-1 SAR IMAGRY

Zway-Gen Twu , I.J. Dowman
University College London
United Kingdom

Commission II, Working Group 4

KEY WORDS: SAR, DEM Accuracy, Range Error, Intersection Angles

ABSTRACT

Various aspects of stereo height determinations from ERS-1 SAR imagery are described in this paper. A pyramidal stereo matching algorithm is applied on an overlapping stereo pair of PRI and RTM imagery. The factors that influence the DEM accuracy are analysed on four different seed points sets. These factors include the ways to select the seed points and the geometric constraint conditions for SAR intersection. With this standard approach of stereo matching an accuracy of 78m can be achieved for a DEM. It is shown that the accuracy of the DEM is closely related to the range errors and hence the intersection angles of the SAR data and that if this error can be controlled a much better DEM accuracy can be obtained. Experimental results produce a rmse of about 17 m for four different data sets.

1. INTRODUCTION

It is of interest today to study the creation of the Digital Elevation Model (DEM) created from the Synthetic Aperture Radar (SAR) for it can provide DEMs in areas which are not easily accessible to other optical sensors. In this field of research, previous work is mainly focused on SIR-B. In particular, Leberl and his group have written many papers to discuss the subject of stereo matching (Leberl,1986a), (Leberl,1986b), and Mercer, (1995) has reported on the use of stereo airborne SAR. But not many papers have been published regarding the DEM derivation from ERS-1 SAR. Compared with SIR-B, ERS-1 gives more accurate orbit header information, thus it should create a better DEM.

An alternative method of creating DEMs from SAR data is interferometry. Stereo SAR is seen as complementary to IFSAR and can be used where interferometry can not be applied. Work has not yet been carried out to analyse the best condition for implementation of stereo SAR.

In UCL, the work on the ERS-1 SAR has been undertaken for a number of years (Dowman et al.,1992a) (Dowman et al.,1993) and useful results have been obtained. The purpose of this paper is to report on an investigation into the production of DEMs from stereoscopic ERS-1 SAR data. In this paper, the pyramidal matching algorithm is introduced and a new strategy is proposed to increase the DEM accuracy tremendously.

2 PYRAMIDAL STEREO MATCHING

Compared with conventional optical imagery, SAR has poor image quality which is affected by layover, noise, and speckle. Thus to stereomatch SAR, there are many problems encountered. To overcome these problems in UCL, a new approach is proposed to implement a coarse to fine pyramidal method. This pyramidal matching is called CHEOPS [named after the Great Pyramid of Cheops at Gizza near Cairo] (Demos,1992). The CHEOPS algorithm is capable of automatically generating the shell scripts required to match both SAR and other forms of imagery. It does this by interpreting a script describing the topology of image pyramids written in a simple language called PDL (Pyramid Description

Language) and then converting this script into an equivalent set of executable UNIX shell scripts. In this paper, the PDL file is defined to use the Otto-Chau stereo matcher for each tier. The Otto-Chau stereo matcher is an area-based patch correlation technique which incorporates the Gruen's Adaptive Least Squares Correlation and a sheet growing algorithm. This stereo matcher performed very well in the SPOT imagery (day and Muller, 1989). The detail of this stereo matcher can be found in (Otto and Chau,1989). For the seed points, the CHEOPS uses the random seed points generated in the first tier of image pyramid. Some research at UCL takes advantage of CHEOPS in dealing with the matching problems in SAR image. Dowman et al., (1992b) first applied CHEOPS on ERS-1 SAR data with different modes and different angles combination. (Demos,1991) implement the CHEOPS on the NASA Seasat satellite images of Death Valley, and tried 9 tiers achieve coverage of 81% over 1024 by 1024 imagery.

3. INTERSECTION

The intersection of ERS-1 SAR in this paper is the analytic approach, proposed by Clark to geocode the SIR-B imagery in her Ph.D. thesis (Clark,1991). The analytic approach primarily utilises two Doppler equations (1) (2) and two range equations (3) (4) to obtain the solution.

$$f_{DC1} = \frac{2(\dot{S}_1 - \dot{P})(S_1 - P)}{\lambda_1 |S_1 - P|} \quad (1)$$

$$f_{DC2} = \frac{2(\dot{S}_2 - \dot{P})(S_2 - P)}{\lambda_2 |S_2 - P|} \quad (2)$$

$$R_1 = |S_1 - P| \quad (3)$$

$$R_2 = |S_2 - P| \quad (4)$$

where image1 and image2 are the stereo pair

f_{DC1} is the Doppler value for image1

f_{DC2} is the Doppler value for image2

R_1 is the range distance in image1

R_2 is the range distance in image2

\dot{S}_1 is the velocity of the sensor for image1

\dot{S}_2 is the velocity of the sensor for image2
 S_1 is the position of the sensor for image1
 S_2 is the position of the sensor for image2
 λ_1 is the radar wavelength for image1
 λ_2 is the radar wavelength for image2
 \dot{P} is the velocity of the target point on the ground
 P is the position of the target point on the ground

In the above four equations, the sensor position and velocity vectors are provided by the header data file in each image. And 3D coordinates of P are unknowns which are solved by the Least Squares iteration technique. From a geometric view, (Curlander,1984) noted that this approach is determined by three faces (1) Earth's shape (2) Doppler equation and (3) range equation. That means, at a particular time, the range equation determined the surface of a sphere, while the Doppler equations described the surface of a cone, the intersection surface of a sphere and a cone yields a circle which is intersected with the Earth model and to give the exact position of a target point.

It should be noted here, that this intersection procedure must be accomplished on the inertial reference system with respect to geocenter. Because the two overlapping images may be taken at different times, the inertial coordinate system for each image may be also different. It is necessary to convert one system to coincide with the other. The conversion factor is related to the GMST (Greenwich Mean Sideral Time) of the system. In order to carry out the intersection we require matching results and header data to provide geocentric coordinate for each terrain point. The intersection procedures include many steps of calculation which are illustrated in the intersection flow chart figure 1.

4 EVALUATIONS OF STEREO MATCHING

In the CHEOPS algorithm, there are many parameters that affect the matching accuracy, from the parameters of generation the seed points to the image tiers used in the matching. In this paper, the evaluation of the matching is based on DEM accuracies. There are four different seed points sets which are used for assessing the matching results for several aspects, which will be discussed in detail separately.

4.1 Data set

The test data in this paper include one ERS-1 precision image (center incidence angle 23°) and one ERS-1 roll-tilt mode image (center incidence angle 35°). This overlapping area covers Marseilles and Aix en Provence in south France. The DEM in this area is also available generated by IGN but part of the overlapping area is not covered by the ground truth. For evaluation of DEM accuracy, 512*512 portion of the overlapping area is extracted.

4.2 DEM accuracies and single image tier accuracy

For the CHEOPS PDL file used in this research the matching results from the preceding tiers are multiplied by the factor 2 and used as initial values in the next tier. Because of this the total DEM accuracy can be estimated by a single image tier. Table 1 illustrates this fact.

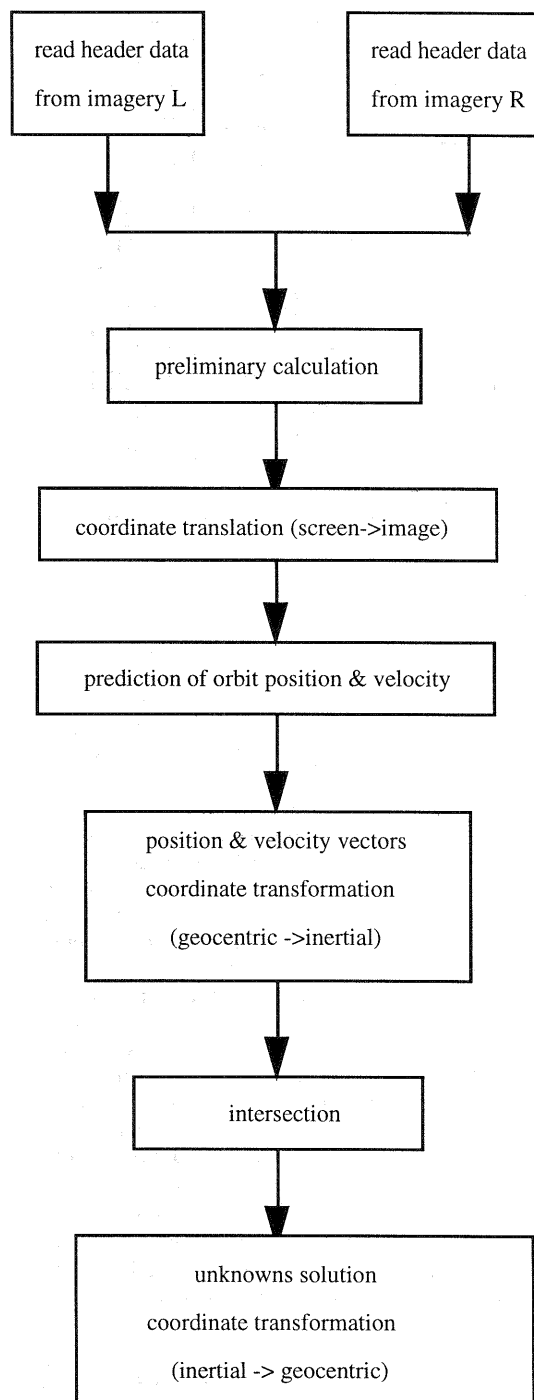


Figure 1: Intersection flow-chart

In table 1, six image tiers were used, the sixth tier is the original image, the fifth tier is reduced by 2 and so on. From this table it is obvious that the total DEM accuracy is strongly influenced by the fifth tier results, for there are about 80% of the matching points on this tier. Also, the table showed that for the ERS-1 SAR imagery, it is better to undertake the matching on the lower resolution of the 5th tier image rather than the original one, this is shown in row 10 that DEM accuracy of tier 6 is lower than any other tiers of image. This also illustrates the benefit of using CHEOPS.

	set1	set 2	set 3	set 4
total*	89.42	90.12	90.01	96.05
No.	40569	40825	40749	40507
tier3*	119.92	130.08	122.96	124.26
No.**	1101	1104	1104	1102
tier4*	80.04	78.57	79.05	80.44
No.**	6871	6873	6871	6875
tier5*	83.58	84.62	84.52	82.90
No.**	31488	31638	31576	31166
tier6*	146.56	131.44	136.44	212.11
No.**	1082	1092	1077	1239

Table 1: Total DEM accuracy and each tier DEM accuracy

* DEM accuracy (meters)

**matching number

4.3 Average of disparity sum and DEM accuracies

In CHEOPS, the seed points are produced randomly in the first tier of image. Accuracy might be improved if we can find a way of selecting the seed points that will have the best final results. An unique object function should be used and many sets of seed points created and the set which gives the best result retained. From table 1 it is concluded that the highest DEM accuracy can be achieved only if the fifth tier DEM accuracy is good. Certainly, it is impractical and meaningless, if we chose the seed points based on the fifth tier DEM accuracy. Dowman et al., (1993) stated that the disparity of the matching results have great impact on the DEM accuracies. And in this research, this conclusion is used as the object function to decide the best seed points. This algorithm is implemented on the third tier, for the seed points are produced in great number (more than 1000) and the calculation time can be accepted. Four different sets of seed points were produced iteratively 1000 times, separately for each set, and those seed points in each set with the smallest Average of Sum Disparity (ASD) were retained. The resulting ASD values on the third tier for the original and smallest one are listed in the table 2 and their DEM accuracies are shown in table 3 for easy comparison.

	set 1	set 2	set 3	set 4
original tier3 *	-0.504	-0.502	-0.501	-0.508
minimum *	-0.486	-0.486	-0.486	-0.486

Table 2: Average and minimum sum disparity for original and smallest one on tier3 for four sets of seed points

*Average of sum disparity (pixels)

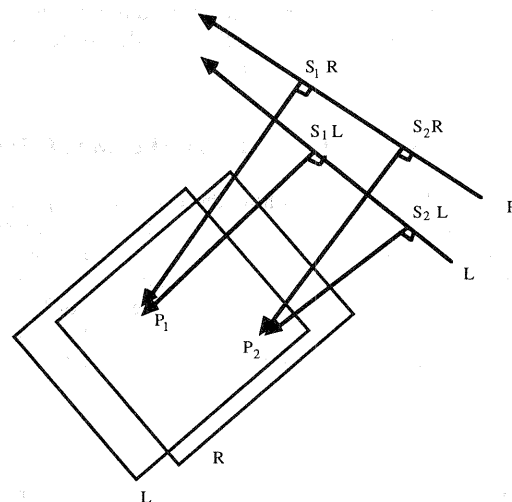
	set 1	set 2	set 3	set 4
original	89.42	90.12	90.04	96.05
smallest ADS	87.39	87.67	88.67	88.77

Table 3: DEM accuracy (m) for original and smallest ADS seed points

In the table 3 the smallest ASD value, the DEM accuracy just increased a little, but it provides another feasible approach to choose the seed points.

5. GEOMETRIC CONSTRAINTS ON ERS-1 SAR INTERSECTION

The equations (1)-(4) give the intersection condition of the ERS-1 SAR. That is, for a single terrain point, it must satisfy these four equations- two Doppler equations and two range equations. And the purpose of this section is to find an unique function to search for the bad terrain points caused by the matching errors based on these four equations. Unfortunately, the two Doppler equations are not useful for most of the matching points satisfy this condition, that is - the velocity vectors of the orbit are perpendicular to the vectors connecting the terrain points and orbit position. In figure 2, this condition is represented by the $S1R1 \perp V1R$ and $S2R2 \perp V2R$. As with the range equations, they are very effective in removing the matching blunders. In this research, the sum of the residuals of two range equations is defined as the range error which is also shown in figure 2. In theory, the smaller the range errors, the higher the DEM accuracy but it is not the case in practice. To more accurately estimate the DEM height errors caused by the range errors, this paper calculates the height errors and range errors for four different data sets. The results are listed in table 4



where P1 and P2 are the any two terrain points from intersection

P1 is the intersection of P1S1L and P1S1R

P2 is the intersection of P2S2L and P2S2R

let S1L: the orbit position for point P1 (left image)

S1R: the orbit position for point P1(right image)

R1L: the range distance for point P1(left image)

R1R: the range distance for point P2(right image)

P1S1L: slant range for P1 (left image)

P1S1R: slant range for P1(right image)

Range error for P1=(P1S1L-R1L)+(P1S1R-R1R)

Same notation for P2

Range error for P2=(P2S2L-R2L)+(P2S2R-R2R)

Figure 2: Geometric condition for ERS-1 SAR

	set 1	set 2	set 3	set 4
height error	*	*	*	*
range error(avg)	5.86	1.85	2.27	-0.36
inter. angle(avg)	14.996	14.991	14.988	14.988
No.	134	169	247	249
height error	**	**	**	**
range error(avg)	-10.43	-10.42	-10.42	-11.13
inter. angle(avg)	15.008	15.009	15.009	15.009
No.	19174	19920	20139	19481
height error	***	***	***	***
range error(avg]	-22.41	-22.59	-22.84	-22.97
inter. angle(avg)	14.997	14.999	15.000	15.000
No.	530	535	539	519

Table 4: Range errors and intersection angles for all different DEM height error

* means the DEM height errors are -500~-250m

** means the DEM height errors are -50~50m

*** means the DEM height errors are 250~500m

It is obviously seen that for each data set the range errors play an important role in determining the height errors. According to the research, for this pair it is best to control range error between -8 ~ -12. Also, the change in range error is proportional to the image coordinate. If one pixel is added in the Y direction, the range error is reduced by 7.9. If one pixel is added in the X direction the range error is reduced by 0.3. From this relationship, it is possible to shift the Y₂ coordinate of each matching point, to control all the range errors to be between -8 ~ -12 and see what they will be like. The results are very encouraging, they do significantly decrease the DEM height error. The table 5 gives the DEM accuracy with or without the range errors control for four different sets, and for each set the DEM accuracy is reduced at least 50m. The success of the range error can be explained by the intersection angles. From the geometric view, for every terrain point, the larger the intersection angle the more accurate the intersection. This conclusion is quite consistent here if we inspect the table 4 again, the intersection angle is the largest one for the height error -50 ~ 50m for all the different four data sets. Changing the range error can also alter the intersection angle simultaneously. That is, to shift the Y₂ coordinate based on the range error is actually to increase the intersection angle and cause very good DEM result.

	set 1	set 2	set 3	set 4
DEM no control	89.42	90.12	90.01	96.05
DEM control	17.12	16.90	16.81	17.26

Table 5: DEM accuracy (m) before or after the range errors control

6. CONCLUSION

From the statistics of the tables in this paper, it is shown that the CHEOPS is a good approach to stereo match the SAR. The benefits of the CHEOPS are analysed. Meanwhile, the function to choose the seed

points are also proposed. The best achievement in this paper is to introduce the idea of range errors which are very effective to enhance the DEM height accuracy. Nevertheless, there is still more work to be done, particularly the performance of CHEOPS on opposite-side imagery should be analysed and the effectiveness of the range errors on that pair should be tested as well. These are all under studies in UCL currently, hopefully, there will be many excellent results published in the near future.

REFERENCES

Clark C., 1991. Geocoding and stereoscopy of SAR. Ph.D. Thesis, University College London

Curlander J.C., 1984. Utilization of spaceborne SAR data for mapping. IEEE transaction on Geoscience & Remote Sensing, 22(2):106-112

Day T., Muller J.P., 1989. Digital elevation model production by stereo-matching SPOT image pairs: a comparison of algorithm. Image and Vision Computing , 7(2):95-101

Denos M., 1991. An automatic approach in stereo matching SEASAT imagery. Proceeding of the British Machine Vision Conference, 335-339

Denos M., 1992. A pyramidal scheme for stereo matching SIR-B imagery. International J. of Remote Sensing, 13(2): 387-392

Dowman I.J., Clark C., Denos M., 1992a. Three dimensional data from SAR Images. International Archives of Proceeding of Remote Sensing 29(4): 425-427

Dowman I.J., Upton M., Knecht J. de, Davison J., 1992b. Preliminary studies on the application of ERS-1 data to topographic mapping. Proceeding of the First ERS-1 Symposium ESA SP-359, pp.543-549

Dowman I.J., Chen P-H, Oclochez O., Saundercock G., 1993. Height from stereoscopic ERS-1 data. Proceeding Second ERS-1 Symposium ESA SP-361, pp. 609-614

Leberl F.W., Domik G., Raggam J., Kobrick M., 1986a. Radar stereomapping techniques and application to SIR-B. IEEE Transaction on Geoscience & Remote Sensing, 24(4): 473-481

Leberl F.W., Domik G., Raggam J., Cimino J., Kobrick M., 1986b. Multiple incidence angle SIR-B experiment over Argentina: stereo-radargrammetric analysis. IEEE Transaction on Geoscience & Remote Sensing, 24(4): 482-491

Mercer J. B., 1995. SAR techniques for topographic mapping . Photogrammetric Week'95 Wichmann. Pp 117-126

Otto G.P., Chau T.K.W., 1989. Region growing algorithm for matching of terrain images. Image and Vision Computing , 7(2):83-94